Inhomogeneous quasi-stationary states in a mean-field model with repulsive cosine interactions

2002 J. Phys. A: Math. Gen. 35 4413

(http://iopscience.iop.org/0305-4470/35/20/303)

INSTITUTE OF PHYSICS PUBLISHING JOURNAL OF PHYSICS A: MATHEMATICAL AND GENERAL

J. Phys. A: Math. Gen. **35** (2002) 4413–4427 PII: S0305-4470(02)30568-7

Inhomogeneous quasi-stationary states in a mean-field model with repulsive cosine interactions

F Leyvraz[1,3], **M-C Firpo**[1,4] **and S Ruffo**[1,2]

[1] Dipartimento di Energetica 'Sergio Stecco', Università degli Studi di Firenze, Via Santa Marta 3, I-50139 Firenze, Italy
[2] INFM and INFN, Firenze, Italy

E-mail: leyvraz@fis.unam.mx, firpo@mit.edu and ruffo@avanzi.de.unifi.it

Received 6 November 2001, in final form 12 March 2002
Published 10 May 2002
Online at stacks.iop.org/JPhysA/35/4413

Abstract

The system of N particles moving on a circle and interacting via a global repulsive cosine interaction is well known to display spatially inhomogeneous structures of extraordinary stability starting from certain low-energy initial conditions. The aim of this paper is to show in a detailed manner how these structures arise and to explain their stability. By a convenient canonical transformation we rewrite the Hamiltonian in such a way that fast and slow variables are singled out and the canonical coordinates of a *collective mode* are naturally introduced. If, initially, enough energy is put in this mode, its decay can be extremely slow. However, both analytical arguments and numerical simulations suggest that these structures eventually decay to the spatially uniform equilibrium state, although this can happen on impressively long time scales. Finally, we heuristically introduce a one-particle time-dependent Hamiltonian that well reproduces most of the observed phenomenology.

PACS numbers: 05.45.−a, 52.35.−g

1. Introduction

Mean-field models, i.e. models in which all the particles interact with equal intensity regardless of distance, have been the object of considerable interest (see [1] for a review and the references therein). One of the simplest models of this kind consists of N particles moving on a circle coupled globally by a cosine interaction [2, 3], with Hamiltonian

$$H = \frac{1}{2}\sum_{i=1}^{N} p_i^2 + \frac{J}{2N}\sum_{i,j=1}^{N} \cos(\theta_i - \theta_j). \tag{1}$$

[3] Permanent address: Centro de Ciencias Fisicas, UNAM, Apdo Postal 48-3, 62251 Cuernavaca, Morelos, Mexico.
[4] Present address: Massachusetts Institute of Technology, Cambridge, MA 02139-4307, USA.

It is sometimes called the Hamiltonian mean-field model (HMF). Here the variables p_i are the momenta conjugate to θ_i, which is the angle describing the state of the ith particle. As stated above, the strength of the interparticle interaction does not depend on the distance and all particles interact with all others. Alternatively, one can think of this model as representing a mean-field approximation to the classical XY model, though this certainly is not a realistic model for a spin system. Its equilibrium statistical mechanics can be treated exactly via the Hubbard–Stratonovich transformation, as shown in [3, 4]. The attractive case, corresponding to $J < 0$, is shown to have a phase transition at a certain value of the inverse temperature $\beta_c = 2/J$, above which the stable state has a *clustered* structure: i.e., the particle density on the circle shows a non-trivial profile. Analogous results were also obtained using entropy maximization methods [5, 6] and, numerically, for a time discrete version of model (1) [7, 8]. On the other hand, in the repulsive case ($J > 0$), no phase transition is found [3]. This can be heuristically justified through the following physical argument. First, note that Hamiltonian (1) can be rewritten as follows:

$$H = \frac{1}{2}\sum_{i=1}^{N} p_i^2 + \frac{J}{2N}\left[\left(\sum_{i=1}^{N}\cos\theta_i\right)^2 + \left(\sum_{i=1}^{N}\sin\theta_i\right)^2\right]. \tag{2}$$

From this it follows immediately that, at least if N is an even number, any state in which all spins appear in pairs $(\theta_k, \pi + \theta_k)$ for all k corresponds to a ground state configuration of the system, all of such states having the same energy. Since the positions of half the angles can be chosen arbitrarily without in any way affecting the energy, uniform ground states will be entropically favoured, thus precluding the appearance of a thermodynamically stable density modulation at low temperatures, as is indeed rigorously established in [3, 4].

It was therefore quite intriguing to find spatially inhomogeneous solutions in the antiferromagnetic case [3, 8–10]. Numerically, they have been found in molecular dynamics simulations starting from certain initial conditions at low temperatures. These so-called *bicluster* solutions show two paired clusters in the density, i.e., particles appear preferentially in correlated positions $(\theta, \pi + \theta)$. These biclusters were found to be extremely stable, though it is of course never easy to decide on numerical ground whether they are simply very long-lived or truly stationary.

This paper addresses the following issues: in section 2, we give a cursory description of the numerical findings concerning the bicluster. In section 3, we show how the N-particle system can be reduced to a system in which the particles are only linked to each other through the common interaction with a *collective mode*. We shall show that this phenomenon is reminiscent of the wave–particle interaction mechanism that governs a large number of plasma physics phenomena [11, 12]. To make this picture even clearer and more quantitative, we show in section 4 how this system can be further reduced to a one-particle time-dependent Hamiltonian. In section 5, we perform a detailed analysis of the one-particle model, showing that several features of the bicluster can be explained in these terms. Finally, in section 6, we present our conclusions.

2. Description of the bicluster

In the following, we consider a system of N particles interacting according to Hamiltonian (1) with a positive value of J, corresponding to repulsion among the particles. We shall consider almost exclusively the following initial conditions: the initial velocities are all identically zero, and the angles are randomly distributed according to a uniform distribution on the interval $[0, 2\pi]$. Since this is not, in general, an equilibrium position, the particles start moving and

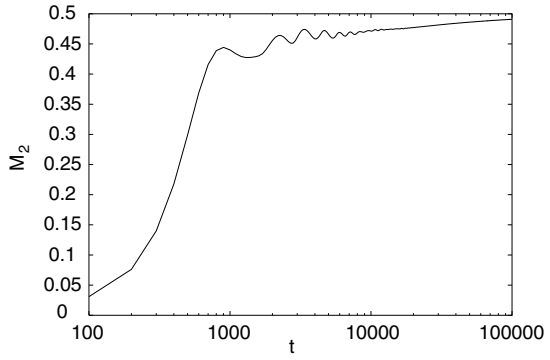

Figure 1. Time dependence of $|M_2(t)|$ for a system of $N = 10^5$ particles at short times.

acquire typical velocities of the order of $N^{-1/2}$. We are therefore always dealing with the low-energy dynamics of the system in the large N limit. Under these circumstances, it is found numerically that a bicluster forms, i.e., the particle density becomes inhomogeneous. The early stages of this formation were studied analytically in [13], using a convenient zero-temperature limit of the Vlasov equation. These involve the rapid formation of rather complex spatio-temporal inhomogeneities, the so-called *chevrons*, which, however, disappear on a fairly rapid time scale. Since we are here primarily interested in the long-time behaviour, these shall not concern us in the following.

Once the initial stages of growth described in [13] are over, an apparently stationary density $\rho(\theta)$ arises. The time evolution of this density can be characterized by the following moments:

$$M_k(t) = \frac{1}{N}\sum_{m=1}^{N} \exp(\mathrm{i}k\theta_m(t)). \tag{3}$$

The second moment $|M_2(t)|$ is shown in figure 1 for a large system ($N = 10^5$ particles). After some oscillations corresponding to the chevron structures described in [13], the second moment eventually reaches a constant value of order one (though on the times shown in the figure, the increase is not yet quite over). Apart from quite rapid oscillations, which we always average over, the density $\rho(\theta)$ settles down onto a provisionally stable profile, the *bicluster*, which is shown in figure 2.

It is found on numerical evidence [10] that the time-averaged moments $M_k^{(0)}$ in this *quasi-stationary state* are well approximated by the expression

$$\left|M_0^{(0)}\right| = 1 \qquad \left|M_{2k}^{(0)}\right| = \frac{1}{|k|} \qquad (k \neq 0) \tag{4}$$

whereas they are zero for odd values of k. This leads to the following analytical expression for the density (again after averaging over the rapid oscillations):

$$\rho_0(\theta) = \frac{1}{2\pi}(1 - \ln|2\sin\theta|). \tag{5}$$

Here the moments $M_k^{(0)}$ and the density $\rho_0(\theta)$ are connected by the following relation:

$$M_k^{(0)} = \frac{1}{2\pi}\int_0^{2\pi} \rho_0(\theta)\,\mathrm{e}^{\mathrm{i}k\theta}\,\mathrm{d}\theta. \tag{6}$$

The bicluster state does not last forever, at least for finite values of N. Indeed, we have performed additional numerical simulations of the system and could observe the decay of the

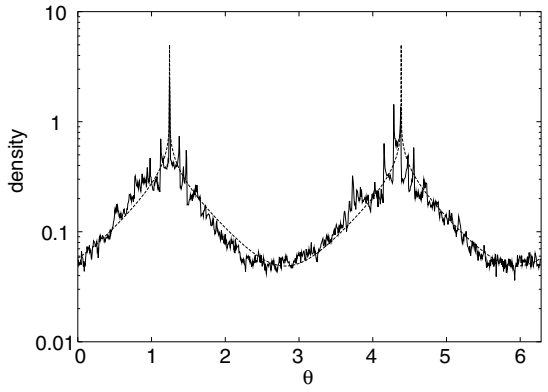

Figure 2. Bicluster density $\rho(\theta)$ for a system of $N = 10^5$ particles. The full line represents the result of numerical experiments, the dashed line represents the theoretical expression (5).

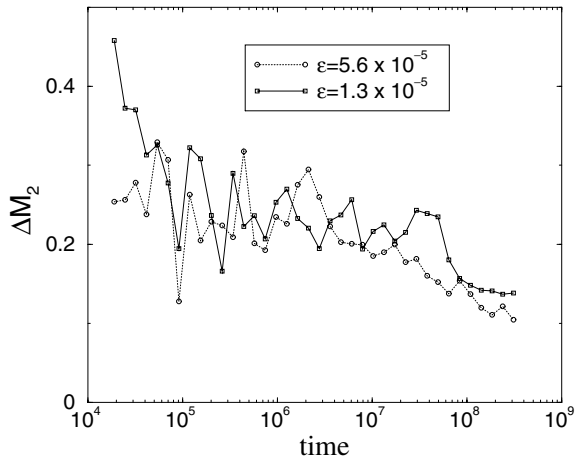

Figure 3. Decay of $\Delta M_2(t)$ ($|M_2(t)|$ minus the finite N equilibrium value) for two systems of 50 particles with different energy densities $\varepsilon = H/N$ in log–linear scale. To smooth out fluctuations, $\Delta M_2(t)$ has been averaged over time intervals of exponentially growing size.

second moment to its equilibrium value over a long time scale. Specifically, for $N = 50$, the relaxation of $|M_2(t)|$ is displayed in figure 3 for two different energy densities. We see that a significant relaxation to equilibrium has taken place by a time of approximately 4×10^8 for both energies. These times rapidly increase as N increases, so that, in some sense, one might argue that the bicluster is some kind of equilibrium state. This is related to the issue of the non-commutation of the limits $t \to \infty$ and $N \to \infty$ in mean-field or Vlasov-like systems (see, e.g., [14, 15] for a numerical approach). On the other hand, the appearance of a bicluster is closely linked to the peculiar choice of the initial conditions: in particular, if instead of starting with zero velocities and random positions, one starts with random velocities of the same order as those that will eventually develop in the former initial condition, no bicluster formation is observed. Together with the fact that we are dealing with a very low-energy phenomenon in a system with long-range forces, this leads us to suspect that the bicluster is simply a phenomenon involving *metastable* configurations. Since it is well known that

metastable states become infinitely long-lived in the mean-field limit, this point of view is in full agreement with the one involving non-commuting long-time and thermodynamic limits.

3. A simple equivalent model

Our purpose in this section is to map Hamiltonian (1) onto a system of the following form:

$$\tilde{H} = \frac{\omega(\phi)^2 P^2}{2NJ} + \frac{NJX^2}{2} + \frac{1}{2}\sum_{k=1}^{N} p_k^2. \tag{7}$$

Here P and X stand for two canonically conjugate variables. The vector ϕ has coordinates ϕ_k, conjugate to the p_k, and $\omega(\phi)$ is a smooth function which will be computed explicitly in the following. Here the ϕ_k correspond to the angles of the original particles, whereas P and X correspond to an explicit separation of a *collective mode*. One therefore has the following situation: the system consists of non-interacting particles coupled to an oscillatory excitation, in a similar way as that familiar in the wave–particle models in plasma physics [11]. Furthermore, as we shall see, the function $\omega(\phi)$ is an average over all ϕ_k, and therefore a slowly varying function. Under these circumstances, one expects a very accurate (though, in general, not exact) conservation of the adiabatic invariant related to the energy stored in the collective mode. As we shall see, if this invariant has an initial value much larger than its thermal average value, a bicluster forms and lasts as long as the invariant maintains its value.

To show this correspondence, we start by considering system (1) as a system of particles in two dimensions, where all the particles are additionally constrained to move on the unit circle. In order to deal with the constraint, it is convenient to go to the Lagrangian formulation. One finds for the Lagrangian corresponding to (1)

$$L = \frac{1}{2}\sum_{k=1}^{N}\left(\dot{\bar{x}}_k^2 + \dot{\bar{y}}_k^2\right) - \frac{J}{2N}\left[\left(\sum_{k=1}^{N}\bar{x}_k\right)^2 + \left(\sum_{k=1}^{N}\bar{y}_k\right)^2\right] + \sum_{k=1}^{N}\lambda_k\left(\bar{x}_k^2 + \bar{y}_k^2 - 1\right). \tag{8}$$

This has the form of a non-linearly constrained N-dimensional harmonic oscillator. We now separate the motion of the centre of mass, since it plays a peculiar role. We therefore introduce

$$X_1 = \frac{1}{N}\sum_{k=1}^{N}\bar{x}_k \qquad X_2 = \frac{1}{N}\sum_{k=1}^{N}\bar{y}_k \qquad x_k = \bar{x}_k - X_1 \qquad y_k = \bar{y}_k - X_2. \tag{9}$$

In these new coordinates the Lagrangian reads

$$L = \frac{1}{2}\sum_{k=1}^{N}\left(\dot{x}_k^2 + \dot{y}_k^2\right) + \frac{N}{2}\left[\dot{X}_1^2 + \dot{X}_2^2 - J\left(X_1^2 + X_2^2\right)\right] + \sum_{k=1}^{N}\lambda_k\left(x_k^2 + y_k^2 + 2X_1x_k + 2X_2y_k + X_1^2 + X_2^2 - 1\right). \tag{10}$$

Going back to polar coordinates and making the following approximations, which are valid in the limit in which the formation of the bicluster is observed,

$$X_1, X_2 \ll 1 \qquad \dot{X}_1, \dot{X}_2 \ll 1 \tag{11}$$

one finally obtains for the Lagrangian, after some manipulations shown in appendix A,

$$L_0 = \frac{\dot{X}^2}{2}\left(N + \sum_{k=1}^{N}\cos^2\phi_k\right) + \frac{N}{2}X^2\dot{\Phi}^2 + \sum_{k=1}^{N}\frac{\dot{\phi}_k^2}{2} - \frac{NJ}{2}X^2. \tag{12}$$

Here X and Φ are related to X_1 and X_2 via

$$X_1 = X\cos\Phi \qquad X_2 = X\sin\Phi. \tag{13}$$

Let us now switch back to the Hamiltonian picture. The Hamiltonian corresponding to (12) is exactly given by

$$H = \frac{\omega(\phi)^2 P^2}{2NJ} + \frac{NJX^2}{2} + \frac{\Lambda^2}{2NX^2} + \frac{1}{2}\sum_{k=1}^{N} p_k^2. \tag{14}$$

Here P is conjugate to X and Λ to Φ. As a final remark, we note that Λ is an exact constant of the motion, namely the total angular momentum. It can therefore always be set equal to zero without loss of generality. This therefore leads us to (7). The frequency function $\omega(\phi)$ is given by

$$\omega(\phi) = \sqrt{\frac{NJ}{N + \sum_{k=1}^{N}\cos^2\phi_k}}. \tag{15}$$

Hamiltonian (7) is very similar in form to those developed in the theory of wave–particle interactions in plasma physics. However, it should be emphasized at this stage that the system described by (7) is still an N-dimensional system. Contrary to the reduction proposed in [11] where bulk and tail (i.e. suprathermal) particles can be discriminated, our system is 'cold' so that all particles participate at the same level to the collective mode.

A very appealing interpretation of (7) is the following. Consider a ring of mass 1 on which N beads of mass $1/N$ can move freely. If X is taken to be the amplitude of the torsional vibrations of such a ring around the y-axis, and if no other motion of the ring is allowed, then (7) describes the motion both of the ring and the beads. Consequently, if we start with particles at rest and with an initial vibration entirely in the degree of freedom associated with the ring, we will have the ring oscillating first around its axis, and then driving the beads towards those regions where the ring motion is least, i.e., towards the two points of the ring lying on the y-axis. Such a structure corresponds exactly to what is observed for the bicluster.

We now proceed with the calculation. Our aim is twofold. On the one hand, we show that equilibrium states do not contain a density modulation. On the other, we display a mechanism capable of leading to very long-lived inhomogeneous states.

Let us first consider the partition function of the effective Hamiltonian (7). The p_k integrals factorize and one is left with

$$Z = \int_0^{2\pi} \mathrm{d}\phi_1 \cdots \mathrm{d}\phi_N \omega(\phi)^{-1} \int \mathrm{d}P\,\mathrm{d}X \exp\left(-\frac{\beta}{2}(P^2 + X^2)\right). \tag{16}$$

This, however, is easily shown not to lead to any density modulation in the angles, since $\omega(\phi)$ is of order one. We must therefore look beyond statistical equilibrium, something already indicated by the plausibility arguments mentioned in the introduction as well as by exact results.

To this end, we transform X and P locally to action-angle variables, i.e., we transform to

$$\begin{aligned} I &= \frac{1}{2}\left(\frac{\omega(\phi)P^2}{NJ} + \frac{NJX^2}{\omega(\phi)}\right) \\ \psi &= \arctan\frac{\omega(\phi)P}{NJX}. \end{aligned} \tag{17}$$

This transformation must be complemented by an appropriate transformation of the ϕ_k to make it canonical. This is computed and discussed further in appendix B. The final Hamiltonian is

$$\tilde{H} = \omega(\phi)I(\phi) + \frac{1}{2}\sum_{k=1}^{N}\left(P_k + \frac{I(\phi)\psi}{\omega(\phi)}\frac{\partial\omega(\phi)}{\partial\phi_k}\right)^2 \tag{18}$$

where the P_k are the new particle momenta after the canonical transformation. They are given by (B.3). Note that the interaction terms, which are linear in the p_k, all average to zero in the fast variables ψ, and the others are of order $1/N^2$. They can, therefore, be accurately taken into account via a perturbative averaging approach. The adiabatic theorem then states that the action $I(\phi)$ is conserved to a high degree of precision and over long time scales. We may therefore construct an approximately stationary state as follows: set an arbitrary value for the action I and, using this now as an *external* parameter, compute the resulting equilibrium state for the ϕ_k.

It should be noted here that recently, using a completely different approach involving multiple time expansion, close results have been derived by Barré *et al* in [16]. We believe that our approach complements their work by seeking to provide some intuition for the physical mechanisms involved in these processes.

If we now take I to have given values in (18) and proceed to compute the Gibbs partition function, we can still eliminate the shifts in the P_k and then factor the resulting integral out. We are then left with

$$Z = \int_0^{2\pi} \mathrm{d}\phi_1 \cdots \mathrm{d}\phi_N \exp[-\beta\omega(\phi)I]. \tag{19}$$

Since $\omega(\phi)$ is of order one, it is necessary for I to be of order N/β (i.e., N times larger than predicted by equipartition) in order to induce a density modulation of order one in the angles. On the other hand, if such a modulation is induced, it is straightforward to verify that it will indeed be a π-periodic modulation directed along the direction in which the collective mode oscillates, and therefore has most of the obvious properties observed in the bicluster. Strictly speaking, however, the microcanonical ensemble should be used in this calculation, which may possibly open a broader range of possibilities, as regions of negative temperature become accessible. For a discussion of these issues, see [16].

As stated in section 2, various initial conditions may or may not lead to the formation of a bicluster. Among those that are successful, there are

(i) initial conditions with equispaced angles and a sinusoidal amplitude velocity perturbation: these initial conditions always yield a bicluster, as they put in an extensive (though very small) value for the action I of the collective oscillation and
(ii) initial conditions with random angles and zero initial velocities: for these it is readily verified that the actions of the collective mode are of order one, whereas the typical velocity of a particle decays as $1/\sqrt{N}$. From this it follows that the effective inverse temperature β increases as N, thus yielding the appropriate result in (19).

4. Reduction to a one-particle model

We here show how to further reduce the model to a one-particle time-dependent Hamiltonian. The assumptions involved are less well controlled and the results we obtain only coincide with the original model over fairly short times. However, in many features, it will turn out that the description given by this simplified model is extremely satisfactory. To this end, we make the following remark: in the model given, say, by (7), all particles are coupled to one single collective mode. The dynamics of this mode is determined both by an external harmonic force and by the reaction forces to all the particles involved. The system is therefore not a one-particle system. In order to reduce it to such a system, we require an approximate expression for the behaviour of the macroscopic mode. Once this is given, a one-particle approximation for the whole system immediately follows. From (7) one obtains

$$\ddot{X} = -\omega^2(\phi)X. \tag{20}$$

Let us now consider the picture of the bicluster developed in section 3. We had found there that the bicluster was a quasi-stationary state in which the action of the collective mode had a given (macroscopic) value and the ϕ a corresponding stationary distribution. From this picture and (20) it follows that, in the bicluster, the motion of the collective mode can be well approximated by a simple harmonic motion.

These observations are confirmed numerically in figure 7 of [10] which shows the phase-points of X_1 in the dynamical regime where the bicluster forms. One can see that X_1 undergoes rapid oscillations of small amplitude around the origin, with its phase only slowly changing in time. Note that, in reality, a slow drift in the relative phase between X_1 and X_2 is actually observed. This is not, however, due to a non-zero value of the angular momentum, but rather to the fact that the description of the motion as a two-dimensional harmonic oscillator is only approximate and not valid over large times.

Armed with this knowledge concerning the dynamics of the collective mode, we can proceed to analyse the behaviour of the particles. We go back to the original θ_k variables. The equation of motion following from (2) can now be rewritten as follows:

$$\ddot{\theta}_k = J[X_1(t)\sin\theta_k - X_2(t)\cos\theta_k]. \tag{21}$$

From this, using the approximate description of the collective mode described above, we obtain the following one-particle approximation:

$$\ddot{\theta}_k = \varepsilon\cos\omega t\,\sin\theta_k. \tag{22}$$

Here the small parameter ε is equal to $J|X_1|$. Note that, by hypothesis, the amplitude of the collective mode $X_1(t)$ is always small, so that this last approximation is in fact justified (see (11)). In the next section we analyse this model in greater detail numerically. Before we do this, however, let us quickly show how this can be treated perturbatively. The dynamics (22) is described by the following Hamiltonian:

$$H = \frac{p^2}{2} - \varepsilon\cos\omega t\cos\theta. \tag{23}$$

Using standard averaging techniques, one finds in the limit of small ε that the motion is well described by the following effective Hamiltonian:

$$\bar{H} = \frac{P^2}{2} - \frac{\varepsilon^2}{8\omega^2}\cos 2\Theta. \tag{24}$$

Here Θ is θ, from which a small rapid oscillation has been subtracted and P is the canonically conjugate momentum. Explicitly

$$\Theta = \theta + \frac{\varepsilon}{2}\left(\frac{\sin(\omega t-\theta)}{(\omega-P)^2} - \frac{\sin(\omega t+\theta)}{(\omega+P)^2}\right). \tag{25}$$

It follows therefore that the particle moves, at least in an average sense, in an effective potential of the form $-\cos 2\Theta$, thereby leading to an attraction to the two points, zero and π.

5. Analysis of the one-particle model

In this section, we investigate numerically whether the dynamical features of the original model (1) with cold initial conditions can be accounted for by the minimal effective model (22) with one-and-a-half degrees of freedom derived in the preceding section. We first observe that we can set $\omega = 1$ without loss of generality, because this parameter can be absorbed in a

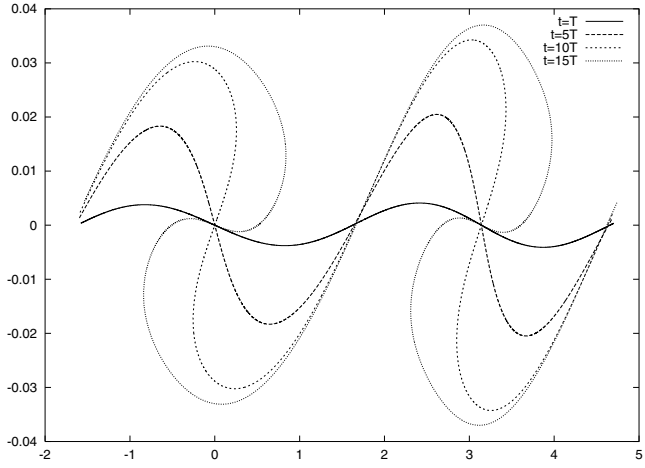

Figure 4. Superposition of one-particle phase-space plots corresponding to the initial points (27), during the initial stage of the bicluster formation. The time unit is the short period $T = 2\pi$.

trivial time rescaling. We then introduce the following area-preserving map with time-step τ, that constitutes the lowest order symplectic algorithm that numerically solves (22):

$$\begin{aligned} \theta_{n+1} &= \theta_n + p_{n+1}\tau \\ p_{n+1} &= p_n - \varepsilon\tau\cos((n+1)\tau)\sin\theta_n. \end{aligned} \tag{26}$$

In order to reproduce the conditions of the simulations performed in [10], we consider a set of N initial conditions featuring a spatially homogeneous distribution of particles of zero momentum. That is, we take for all j, $1 \leqslant j \leqslant N$

$$\theta_0^j = j\frac{2\pi}{N} \quad \text{and} \quad p_0^j = 0. \tag{27}$$

We then compute the resulting N trajectories, obtaining their superposed phase-space plots in figures 4 and 6. Since $\omega = 1$ the period T of the rapid oscillations of the collective variable X_1 takes the value $T = 2\pi$. In these simulations, we fix the time-step $\tau = T/100 = 2\pi/100$ and $\varepsilon = 0.05$. Figure 4 shows the superposed phase-space plots of the N trajectories (27) during the initial stage from which the bicluster structure emerges. All trajectories wind around the elliptic fixed points $\theta = 0, \pi$. In figure 5 we plot some trajectories with initial value $|\theta_0| < \pi/2$, which show rapid oscillations of period T superposed on a much slower oscillatory motion around the minimum in $\theta = 0$ of the time-averaged potential $-\cos 2\Theta$ in Hamiltonian (24). The large time plots of figure 6 clearly reproduce the features of the full HMF N-degrees of freedom phase-space plots (e.g. figure 4 in [10]). The bicluster structure exhibits an overall oscillation on the period T around the zero-momenta fixed points $\theta = 0$ and $\theta = \pi$.

It is also possible, using the effective Hamiltonian (24), to get at least a qualitative understanding of the behaviour of the position and momentum density functions, in particular of their singularities. Indeed, if we assume that all the particles start from rest and are randomly distributed on the unit circle, we find for the density $\rho(\theta)$

$$\rho(\theta) = (2\pi Z)^{-1}\int_0^{2\pi} \mathrm{d}\theta_0 \int_{-\infty}^{\infty} \mathrm{d}p\,\delta[\bar{H}(\theta, p) - \bar{H}(\theta_0, 0)] \tag{28}$$

where Z is the microcanonical phase-space volume and where we have neglected the difference

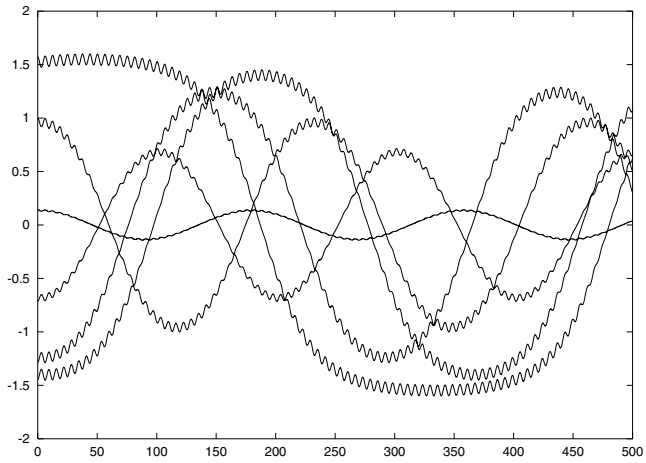

Figure 5. Some trajectories $\theta(t)$ of the one-particle system.

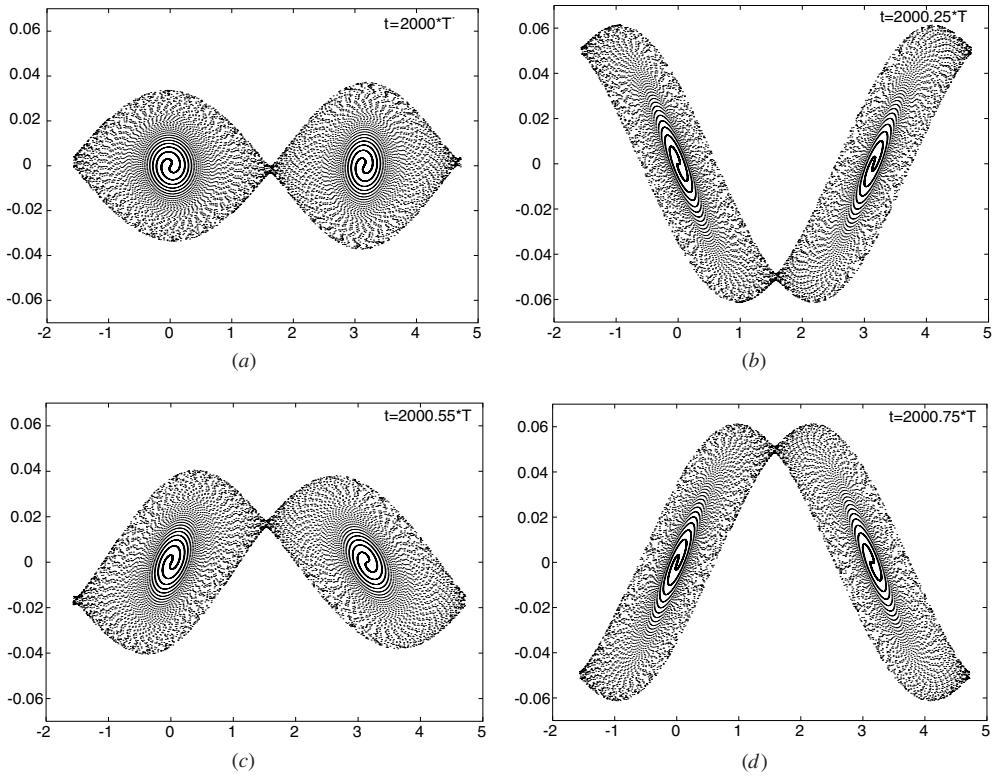

Figure 6. Four snapshots at long-time within the short period $T = 2\pi$ of the phase-space plots of the N trajectories (27). The particle positions have been brought by periodicity to the interval $[-\pi/2; 3\pi/2]$.

between the transformed variables and the original ones. The integral in (28) can be evaluated explicitly to yield

$$\rho(\theta) = \mathcal{N} K(\cos^2\theta) \tag{29}$$

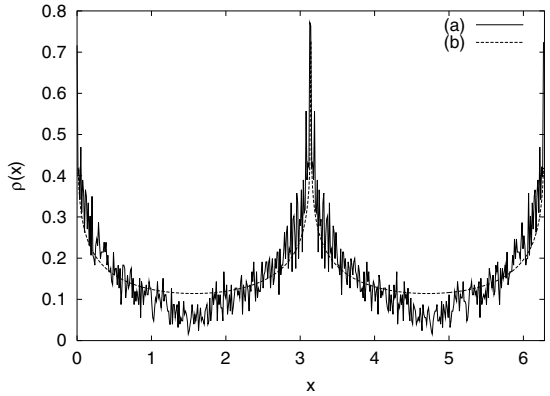

Figure 7. Position density $\rho(\theta)$ at time $t = 2000T$ of the bicluster (a) from the numerical integration of (26) with the 'cold' initial conditions (27) (full line) and (b) from the theoretical prediction (29) (dashed line).

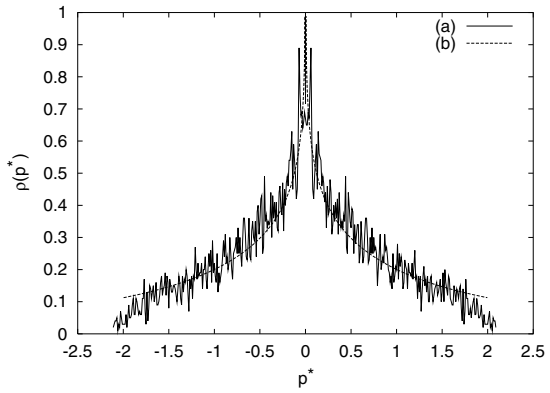

Figure 8. Density of the rescaled momentum $p^* = p/\sqrt{\varepsilon^2/(8\omega^2)}$ at time $t = 2000T$ in the bicluster (a) from the numerical integration of (26) with the 'cold' initial conditions (27) (full line) and (b) from the theoretical prediction (30) (dashed line).

where $K(m)$ is the complete elliptic integral of the first kind as a function of the parameter m and $\mathcal{N}$ is an appropriate normalization constant. The properties of the approximate solution (29) are very similar to those observed for the full N-body system, e.g. we can reproduce the logarithmic singularities at $\theta = 0, \pi$. The general shape is also similar (see figure 7), but the agreement is not as satisfactory as that of the empirical formula (5), shown in figure 2.

A similar calculation for the momentum density yields

$$\rho(p) = \mathcal{N} K\left(1 - \frac{w^4}{16}\right) \qquad (|w| \leqslant 2) \tag{30}$$

where w is the appropriately scaled momentum $p/(\varepsilon^2/8\omega^2)^{1/2}$. Again, this has roughly the right form (see figure 8), but, quantitatively, it is not quite satisfactory.

Model (22) seems therefore to be a good representation of the dynamics of the antiferromagnetic HMF at vanishing energy, even if the assumption of a constant frequency $\omega := 2\pi/T$ is (slightly) violated due to self-consistency in the real system.

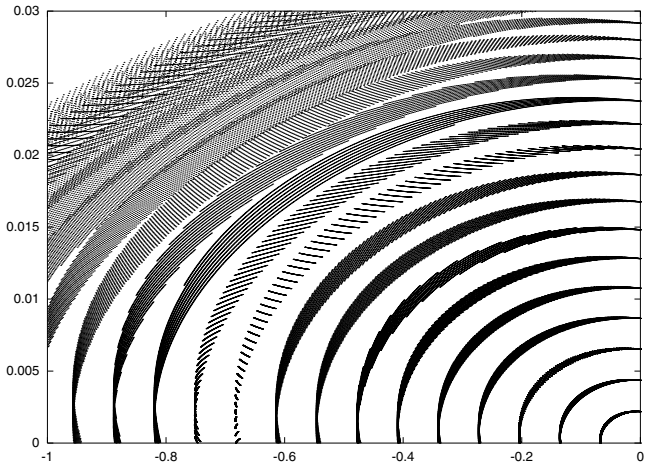

Figure 9. Magnification of a long-time Poincaré plot of system (22) corresponding to orbits of increasing energy around the elliptic point $\theta = p = 0$.

Let us now show that, although simple, this model has a non-trivial dynamics. First note that KAM theorem, which guarantees the preservation of quasiperiodic motions under small perturbations, cannot be applied in its classical form to this system. Renaming the time t as a phase variable φ, the dynamics (22) derives from the two-degrees-of-freedom Hamiltonian

$$H(\theta, p, \varphi, u) = \tfrac{1}{2}p^2 + u - \varepsilon \cos\omega\varphi \cos\theta \tag{31}$$

where the variable u is conjugated to time φ and does not appear in (22). KAM theorem requires a non-degeneracy condition on the frequency vector $\boldsymbol{\omega} := (\partial_p H, \partial_u H)$ to ensure that a large set of actions (p, u) has 'sufficiently irrational' frequencies. This condition is $\det\left(\partial_{(p,u)}\boldsymbol{\omega}\right) \neq 0$. This is trivially not satisfied here as $\boldsymbol{\omega} = (p, 1)$. Yet, within the theory of averaging, KAM theory may be applied to an averaged Hamiltonian exponentially close to (24) with the result that, for ε small enough, the Poincaré section of $\bar{H}$ is filled up to a residue of exponentially small measure by invariant curves that are close to the level lines of $\bar{H}$ [17, 18]. This appears to be confirmed numerically, although in a rather unexpected fashion. Figure 9 displays the enlargement of a long-time Poincaré plot with initial conditions equally spaced on the θ-axis and $\varepsilon = 0.05$. Over the time scales probed by the simulation (4×10^7 time-steps), the particle does not visit the whole phase space, but remains within a well-defined region in agreement with KAM predictions. In this region, however, it appears to lie on an extremely convoluted but smooth invariant surface. Indeed, the Poincaré surface shows a dense pattern of parallel lines on which the points lie. These presumably represent the intersection of a very high order torus with the Poincaré surface. Such behaviour is certainly peculiar, but may well be related to the degenerate nature of the unperturbed system. From this it follows, in this particular case, that no short periodic orbits can exist in this part of the phase space.

If this picture is correct, the system is not ergodic. This then strongly suggests that, in this reduced one-particle model, the bicluster structure lasts forever. The relevance of this conclusion for the N-particle system, however, remains an open question. It is, in principle, conceivable that, among the class of initial conditions we consider, a non-vanishing measure lies on some invariant surface of the N-particle system. However, this certainly does not follow from our previous arguments concerning adiabatic invariance, which only holds over

very long, but not over infinite times. Furthermore, the simulations discussed in section 2 speak against such a possibility.

6. Conclusions

Summarizing, we have found a physically appealing approximate description of the low-temperature dynamics of the repulsive Hamiltonian mean-field model in terms of free particles on a ring performing torsional vibrations. The physical analogue of the ring oscillation is the collective plasmon oscillation of the variables X_1 and X_2. The interaction between particles and ring arises solely from the influence of the particle positions on the moment of inertia of the ring. This provides a straightforward interpretation of the clustering phenomena observed in previous work: if the initial condition is such that the initial ring oscillation strongly dominates the motion of the individual particles, then a parametric instability sets in, driving the particles towards the part of the ring which is at rest. This creates, as shown in section 4, an effective potential of the form $-\cos 2\Theta$ in which the particles move. This same picture can also be used to obtain a description of the statistical mechanical equilibrium. In this case, it is clear that no clusters form, either in the canonical or in the microcanonical ensemble. Furthermore, this effective potential allows us to form a qualitatively correct picture of the particle density, both in position and in momentum space, though clear discrepancies remain, showing that the time-dependent nature of the problem is essential. Finally, we studied the chaotic properties of the time-dependent effective model. For a small, yet finite, modulus of the collective plasmon variable, this model was shown to present localization on very high order tori, and hence lack of ergodicity. This localization is presumably inherent to the small dimension of the system and might not occur in the finite N-particle model. Indeed, even if the tori present in the effective one-particle system actually survived in the N-particle system, Arnold diffusion might still act as a process that would eventually drive the system towards thermal equilibrium.

Acknowledgments

MCF thanks the European Commission for support through a Marie Curie individual fellowship contract no HPMFCT-2000-00596. This work was partially funded by grant IN112200 of DGAPA as well as CONACYT grant number 32173-E. Finally, we acknowledge financial support from INFN, the University of Florence and the MURST-COFIN00 project 'Chaos and localization in quantum and classical mechanics'.

Appendix A. Derivation of the approximate Lagrangian

We start from (10). We now introduce polar coordinates as follows:

$$x_k = \rho_k \cos\phi_k \qquad y_k = \rho_k \sin\phi_k. \tag{A.1}$$

Here the angles ϕ_k are measured from the vector (X_1, X_2). From this it follows readily via the cosine theorem that

$$\rho_k^2 + X^2 - 2X\rho_k \cos\phi_k = 1 \tag{A.2}$$

where X is defined as the norm and Φ as the angle of the vector (X_1, X_2). Within the approximations stated in (11), this yields

$$\rho_k = 1 + X\cos\phi_k. \tag{A.3}$$

From this it follows for the velocities

$$\dot{\rho}_k = \dot{X}\cos\phi_k - X\dot{\phi}_k \sin\phi_k = \dot{X}\cos\phi_k \tag{A.4}$$

where again the last equality uses (11) and $\dot{X}_1, \dot{X}_2 \sim \dot{\phi}_k$. The Lagrangian (10) now reads

$$L = \frac{1}{2}\sum_{k=1}^{N}\left(\dot{\rho}_k^2 + \rho_k^2\dot{\phi}_k^2\right) + \frac{N}{2}[\dot{X}^2 + X^2\dot{\Phi}^2 - JX^2]. \tag{A.5}$$

Substituting (A.3) and (A.4) into (A.5) and using systematically the approximations (11) yields the desired result.

Appendix B. Transformation to action-angle variables

In this appendix, we compute the canonical transformation that generates the local transformation to action-angle variables (17). We shall do this by computing its generating function as follows: we first determine a function $S_0(I, X; \phi_k)$ such that the conditions

$$\frac{\partial S_0}{\partial I} = \psi \qquad \frac{\partial S_0}{\partial X} = P \tag{B.1}$$

are equivalent to (17). This is simply the generating function of the transformation to action-angle variables of the harmonic oscillator, where the ϕ_k enter merely as parameters. If we now define

$$S(I, X; \phi_k, P_k) = \sum_{k=1}^{N} P_k\phi_k + S_0(I, X; \phi_k) \tag{B.2}$$

this determines in the usual way a canonical transformation on the whole space. To compute it explicitly, note that S_0 depends only on the combination $\omega(\phi)I$, so that

$$\begin{aligned} p_k &= P_k + \frac{I\psi}{\omega(\phi)}\frac{\partial\omega(\phi)}{\partial\phi_k} \\ &= P_k + \frac{I\psi}{\omega(\phi)}\cos\phi_k\sin\phi_k\sqrt{\frac{NJ}{\left(1+\sum_{l=1}^{N}\cos^2\phi_l\right)^3}}. \end{aligned} \tag{B.3}$$

Note that these correction terms are of order $1/N$.

References

[1] Antoni M, Ruffo S and Torcini A 2000 *The Chaotic Universe* ed V G Gurzadyan and R Ruffini (Singapore: World Scientific) p 467
[2] Ruffo S 1994 *Transport, Chaos and Plasma Physics* vol 1 ed S Benkadda, F Doveil and Y Elskens (Singapore: World Scientific) p 114
[3] Antoni M and Ruffo S 1995 *Phys. Rev.* E **53** 2361
[4] Latora V, Rapisarda A and Ruffo S 1999 *Physica* D **131** 38
[5] Inagaki S 1993 *Prog. Theor. Phys.* **90** 577
[6] Inagaki S and Konishi T 1993 *Publ. Astron. Soc. Japan* **45** 733
[7] Konishi T and Kaneko K 1992 *J. Phys. A: Math. Gen.* **25** 6283
[8] Kaneko K and Konishi T 1994 *Physica* D **71** 146
[9] Zheng Zhigang and Li XiaoWen 1999 *Commun. Theor. Phys.* **32** 367
[10] Dauxois T, Holdsworth P and Ruffo S 2000 *Eur. Phys. J.* B **16** 659
[11] Antoni M, Elskens Y and Escande D F 1998 *Phys. Plasmas* **5** 841
[12] Timofeev A V 1997 *Plasma Phys. Rep.* **23** 989

[13] Barré J, Dauxois T and Ruffo S 2001 *Physica* A **295** 254
[14] Latora V, Rapisarda A and Ruffo S 1999 *Phys. Rev. Lett.* **83** 2104
[15] Firpo M-C, Doveil F, Elskens Y, Bertrand P, Poleni M and Guyomarc'h D 2001 *Phys. Rev.* E **64** 026407
[16] Barré J, Bouchet F, Dauxois T and Ruffo S 2002 *Preprint* cond-mat/0203013 (*Eur. Phys. J.* B, submitted)
[17] Neihstadt A 2001 Private communication
[18] Treschev D 1996 *Chaos* **6** 6